Tikrit Journal of Engineering Sciences

TJES Tikrit Journal of Engineering Sciences

Open Access

Article

Surface Response Optimization for Absorption of CO_2 Bubbles in Sweetener Solution by the Gas-Liquid Mass Transfer Operation

Ahmed Dheyaa Nsaif*, Ibtehal Kareem Shakir

Chemical Department, Engineering College, Baghdad University, Baghdad, Iraq.

Emails:
Ahmed Dheyaa Nsaif: ahmed.nasif1507d@coeng.uobaghdad.edu.iq , Ibtehal Kareem Shakir: ibtehal.kareem@coeng.uobaghdad.edu.iq

Abstract:

There is a trend to produce soft drinks with new specifications by increasing the amount of carbon dioxide absorbed in them but within the permissible food specifications limits. The experimental investigation of physical absorption was conducted in a bubble column to determine carbon dioxide absorption yield (Y_{CO2}) and volumetric mass transfer coefficients (Kla) to the liquid phase. The aim was to quantify the impact and optimization of the gas diffuser pore size, absorbent solution's temperature, gas flow rate, sucrose concentration, and their interaction on the responses of Y_{CO2} and Kla. Box-Behnken design (BBD) in response surface methodology (RSM) is selected to determine this relationship. The Pareto chart was used to determine the experimental variables significantly impacting the observed responses. According to the analysis of variance (ANOVA), the absorbent solution's temperature, gas diffuser pore size, and sucrose concentration were important process variables that affect the absorption yield of carbon dioxide. All variables with interactions were found to affect volumetric mass transfer coefficients. The optimal responses for maximum Y_{CO2} and Kla were 49.2 % and 0.455 1/min, respectively. The operational conditions were as follows: pore size of the diffuser (0.5 µm), gas flow rate (0.68 L/min), the temperature of absorbent (5 °C), and sucrose concentration (150 g/L).

Keywords:

Absorption; Box–Behnken design; Bubble column; Carbon dioxide; Gas diffuser; Volumetric mass transfer coefficients.

Highlights:

- Absorption of pure CO2 in sweetener solution.
- Studying the effect of gas flow rate, temperature, size of pore diffuser, and sucrose concentrations.
- Calculating the volumetric mass transfer coefficient on the liquid side.
- Response Surface Methodology, Box–Behnken design for optimization operation conditions.

Article History:

Received:	30	Dec.	2023
Received in revised form:	17	Feb.	2024
Accepted:	14	Jun.	2024
Final Proofreading:	16	Apr.	2025
Available online:	05	May	2026

https://doi.org/10.25130/tjes.33.1.10

Citation:

Nsaif AD, Shakir IK. **Surface Response Optimization for Absorption of CO2 Bubbles in Sweetener Solution by the Gas-Liquid Mass Transfer Operation**. *Tikrit Journal of Engineering Sciences* 2026; **33**(1): 1951.

Corresponding Author*:

Ahmed Dheyaa Nsaif
Chemical Department, Engineering College, Baghdad University, Baghdad, Iraq.
Email: ahmed.nasif1507d@coeng.uobaghdad.edu.iq

1.INTRODUCTION

There is a trend to produce an ever-wider range of more specialist soft drinks, and there is also pressure to minimize the use of, in particular, artificial additives and ingredients. Modern soft drinks constitute a diverse group of products. They can be classified in several ways, for example, based on their sugar and fruit juice content, flavoring, carbonation level, main nonwatery ingredients, and functionality. Conventional soft drinks contain 90 % water, while diet soft drinks may contain up to 99 % water. As well as sweetener (8 - 12% w/v), carbon dioxide (0.3 - 0.6% w/v), acidulants (0.05 - 0.3% w/v), flavorings (0.1 - 0.5% w/v), colorings (0 - 70 ppm), chemical preservatives (lawful limits), antioxidants (<100 ppm), and/or foaming agents (e.g., saponins up to 200mg/mL) [1]. Gas-liquid mass transfer is a phenomenon frequently seen in various industrial processes, including chemical, biological, and environmental fields [2-4]. The study of mass transfer in gas-liquid systems is a fundamental area of focus in chemical engineering, with applications spanning industrial and laboratory settings [5-7]. As a result, it is important to assess the volumetric mass transfer coefficients or the specific interfacial areas at the laboratory scale. According to the Stocks equation, the terminal velocity of bubbles is influenced by various factors, including the bubbles' size, shape, and terminal velocity, as well as the density and viscosity qualities of the fluid in both phases [8-11]. The degree of liquid contamination and temperature are just a few variables that affect YCO2 and Kla [8, 12]. In engineering, it is well accepted that the mass transfer from the interface between two fluids into either fluid phase may be accurately described and predicted using equations of a specific form [13]. Many scientists have investigated carbon dioxide capture and storage as a means of reducing the global warming phenomenon [14, 15]. Various techniques available are for capturing carbon dioxide, with aqueous carbon dioxide absorption being recognized as the most efficient approach. Therefore, much research has been conducted to explore various absorbents that might improve the efficiency of carbon dioxide collection. This efficiency is limited by the mass transfer phenomenon between the gas and liquid phases [16]. According to Higbie's equation, the mass transfer coefficients in rising bubble streams with 10% carbon dioxide in the air occurred consistently with what should occur for diffusion in transient films in an uneven condition [13, 16]. Experiments used the following systems: ethanol-water, methanol-water, methanol ethanol, benzene hexane, and benzene toluene in a batch-packed bed distillation column. Multiple regression analysis in a correlation estimates the overall mass transfer coefficient of vapor and liquid phases (KOV and KOL). The correlation relationships were as follows: $KOL= 2.8 \times 10^{-6}\alpha^{-0.95}(DV/ DL)^{0.03}(L / V)^{1.15}(\rho V/\rho L)^{0.077}(\mu V/ \mu L)^{-0.9}$ and $KOV= 3.3 \times 10^{-10}\alpha^{-0.7}(DV/ DL)^{0.65}(L / V)^{3.5}(\rho V/\rho L)^{1.25}(\mu V/ \mu L)^{-5}$ [17]. Carbon dioxide in mono ethanol amine solution (MEA) was recovered experimentally using a prototype plant comprising a perforated sieve tray column. Multiple variables, including MEA concentration, gas phase carbon dioxide ratio, liquid flow rate, gas flow rate, and CO2 loading in the absorption solution, were studied due to their impact [18]. The Kla was computed using air and CO2 in water and NaOH; the column diameter was 0.1 m. It contains a gas dispenser with 79 holes and a diameter of 2 mm per slot for experiments. The mass transfer coefficient was predicted using empirical and ANN correlations in dimensionless groups (Sh, Re, Bo, and We). The results showed an increase in the kL.a with the volumetric gas flow rate and an increase in the concentration of NaOH and e gas-liquid bubble interfacial area (a) between the gas and the liquid [19]. Utilizing a continuous bubble column scrubber for carbon dioxide capturing focused on the impact of operating temperature, pH, and gas-liquid flow on the quantity of carbon dioxide (CO2) absorbed and the overall mass transfer coefficient within a sodium hydroxide (NaOH) solution. The gas flow rate and pH value significantly influenced NaOH absorption, while the operating temperature and liquid flow rate were minimal [20]. The solubility and diffusion of carbon dioxide in seawater and distilled water at different temperatures and pressures are an optimal way to store carbon dioxide in the ocean. Its high solubility at high pressure lessens the total solution time. As temperature rises, diffusivity increases, decreasing the solubility and diffusion of carbon dioxide. Seawater's lesser solubility makes CO2's total solution time longer than in pure water [21]. Various types of water, including saltwater, brackish, reverse osmosis, and purified water, were tested for CO2 absorption and desorption using a bubble column contactor. The absorption and desorption trials indicated that kLa dropped with salinity until a “threshold” value was reached, then increased again. Adsorption kLa values decreased approximately linearly with water alkalinity; however, desorption kLa values showed no patterns [22]. Inkeri and Tynjälä [23] found a simple model to predict the main trends in hydrodynamics and gas-liquid mass transfer in a bubble column reactor. The CO2 capture efficiency, CO2 concentration in product gas, and produced CO2 mass flow were significantly influenced by the gas and liquid inflow rates. High levels of CO2 can be obtained in the gas product using low gas inflow

rates, however, increasing energy consumption. A High liquid flow rate improved CO2 collection efficiency; however, it reduced CO2 content in the final gas. As the incoming gas and liquid flow rates increased, the total rate of CO2 production also increased. Xiaofei et al. [24] determined the effect of fluid viscosity on the rising dynamics of single CO2 bubbles in polyacrylamide aqueous solutions of different weight percentages. Matsuo [25] studied the rising dynamics of single CO2 bubbles in polyacrylamide aqueous solutions of different weight percentages. The effects of PH and bubble diameter on the enhancement factor were studied by measuring single CO2 bubbles as they rose through a pipe containing a NaOH solution. The ratio of kL with and without chemical absorption, E, was nearly one for pH < 12.25. At pH > 12.25, E and d increased. Its magnitude was lower than the two-film theory estimated. The E-correlation was created. Combining the E correlation with Sherwood number correlations for bubbles without chemical absorption resulted in a reliable Sherwood number estimated for bubbles with chemical absorption. The correlations were also applied to larger pipe-diameter bubbles. The mass transfer coefficient of contaminated water is lower than that of pure water. This coefficient diminishes as the surfactant increases concentration, initiating a rise in velocity that impacts the mass transfer rate and transition to the immobile bubble surface. Surfactants affect smaller, slower-rising bubbles more, which can lower the transition Re and cause the immovable bubble surface to develop earlier and lower kL [26]. Carbon dioxide absorption studies were conducted in a packing column with two different types of packing, i.e., Gempak 4A and Raschig ring, to compare them using aqueous solutions and investigate the impact of operational parameters. The solvents used were methyldiethanolamine (MDEA), 2-amino-2-methyl-1-propanol (AMP), diethanolamine (MEA), and diethanolamine (DEA). The absorption efficiency can be measured by the mass transfer coefficient. The mass transfer coefficients of various packings evaluated significantly varied not only with operational parameters, such as liquid load, liquid CO2 loading, solvent concentration, solvent type, and feed CO2 concentration, but also with packing arrangement [27]. The volumetric mass transfer coefficient (Kla) increased with increasing stirrer speed. Thus, bubble dispersion improved with speed, which enhanced the surface-to-volume ratio and mass transfer area (Kla) [28]. The absorption of carbon dioxide gas in a bubble tower was studied using solutions of MEA (monoethanolamine) and alkaline solvents (NaOH, KOH, and Mg(OH)2) with countercurrent flow. The concentration and type of solvent were studied, and the results showed that Mg(OH)2 was less efficient at absorbing CO2 than KOH, NaOH, and MEA. High solvent concentration increased the total mass transfer coefficient, absorption rate, and CO2 removal efficiency across all solvent types [29]. Experimentally and theoretically, The chemical absorption of carbon dioxide and nitrogen mixtures using aqueous ammonia solutions was investigated under operation conditions that included temperature and the concentration of the absorbent. The proportion of carbon dioxide in the combination was fifteen percent by volume, and the results agreed with the experimental and theoretical estimates [30]. The present study aims to produce soft drinks with new specifications by increasing the amount of carbon dioxide absorbed in them, however, within the permissible food specifications limits. The gas-liquid mass transfer phenomenon within a bubble column was investigated to reach this aim. The study examined the effect of the pores diffuser size (0.5 to 500 µm), liquid temperature (5 °C to 25 °C), concentration of sucrose (0 to 150 g/L), and gas flow rate (0.2 to 0.7 L/min) on Y_{CO_2} and the volumetric mass transfer coefficient. Statistical analysis based on the Box-Behnken experimental design is used to predict the relationship between experimental variables and the desired response of yield CO2 absorbent and volumetric mass transfer coefficient. The linear, square, and interactive effects of experimental variables on responses were analyzed to evaluate the second-order equation between the input experimental variables and the achieved response surfaces.

2.MATERIALS AND MEASUREMENTS

2.1.Materials

The CO2 and N2 gases used in the experiments were from Al-Mansour State Company, with a high purity of 99.9%. In addition, the water used in the experiments was RO water from the same company. Food sugar (sucrose, C12H22O11) was used to prepare the solution used in the experiments. The sample solution was 1.75 liters of RO water plus sucrose.

2.2.Measuring CO2 Solubility

Multiple methods can be employed to determine the solubility of carbon dioxide gas in solutions. One approach involves utilizing the principle of mass balance to quantify the dissolved gas by contrasting the mass of gas entering the system with the mass leaving it. The difference between them indicates the quantity of gas dissolved. Mass flow controllers from international manufacturers were used to obtain the highest accuracy of measurement [31].

2.3.Determinating the Overall Coefficient of Mass Transfer Based on the Liquid Side Per Unit Volume (Kla) and Carbon Dioxide Yield

Analogously to the equation that governs the rate of diffusion in gases, it is customary to establish a rate equation for diffusion in liquids, which takes the following form [26]:

$$Nv = Kla\ (C^{*} - C^{L}) \quad (1)$$

The efficacy of mass transfer depends on the interfacial area (a) and gas-liquid interface properties. Gas side mass transfer resistance can be ignored for gases with low liquid phase solubility, such as CO_2 in water. Eq. (1) describes the mass transfer rate in the liquid phase. The mass transfer coefficient in the liquid phase is symbolized by kl, and the interface between the two phases is represented by a. CL is a solute-dissolved concentration, and C* is the saturation concentration of the gas. Henry's law can be used to compute C*[26]. According to Eq. (2), the carbon dioxide yield is the ratio of CO2 absorbed by the solution to the total amount of CO2 gas.

$$Y_{CO_2}\% = Wt_{CO_2\ absorb} / Wt_{CO_2\ total} * 100 \quad (2)$$

where $Y_{CO_2}\%$ is the carbon dioxide yield, $Wt_{CO_2\ absorb}$ is the final weight of the CO_2 absorbed by the liquid, and $Wt_{CO_2\ total}$ is the total weight of CO_2 gas inlet to the process. The volumetric mass transfer coefficient is calculated by integrating Eq. (1) and yields:

$$Ln\ (C^{*} - C^{L}) = -\ Kla * t + constant \quad (3)$$

The value of Kla was calculated from Eq. (3). The slope of the natural logarithm of the difference between the concentration of CO2 in the liquid phase at saturation state and the concentration of CO2 at any time was plotted against time for each experimental run. Evaluating Kla using this method was predicated on two assumptions. The liquid phase exhibited complete homogeneity due to thorough mixing. The driving force for mass transfer exhibited uniformity across the whole column.

3.RESPONSE SURFACE METHODOLOGY

Response surface methodology (RSM) is employed to optimize the experimental variables and evaluate their correlation with the designed responses [32-33]. The response surface methodology is considered an important factor for researchers to reduce the number of experiments, find the optimal conditions, find the relationship between the independent variables, and control the dependent variables by building a mathematical model that describes the process. In this study, based on the response surface methodology, Box-Behnken design (BBD) was used to design several experiments and build models, study the interactive effect of process variables, and obtain optimal operating conditions for the optimization absorption process. The experiment was designed using RSM based on BBD with three continuous independent variables. Each variable was set at three levels (-1, 0, +1) within the specified ranges, and one category independent variable was set at three levels. The responses comprised Yco2 and Kla. The second-order polynomial of Eq. (4) approximates the mathematical relationship between the experimental variables and response [33].

$$(Y_{CO_2}\ and\ Kla) = a_o + \Sigma a_i X_i + \Sigma a_{ii} X_i + \Sigma a_{ij} X_i X_j \quad (4)$$

When Y_{CO_2} and Kla are the predicted response by the mathematical model, X_i and X_j are the independent variables. , a_o is the equation constant, and ai, a_{ii}, and a_{ij} are the regression coefficients of the model. According to Eq. (5), variables are coded for statistical computation.

$$X_i = U_i - U_o / \Delta U_i \quad (5)$$

In this context, Xi is the coded value of the independent variable, Ui is the real value of the independent variable, Uo is the real value of the independent variable at the center point, and ΔUi represents the step change value. The 'MINITABTM' (version 18) software is used for regression analysis of experimental data and response. The regression coefficient R^2 and F-test were used to determine its statistical significance and convey the quality of the fit of the multiple regression model. A student's t-test is used to evaluate the significance of the regression coefficient.

4.EXPERIMENTAL PROGRAM

4.1. Apparatus Description

The experimental measurements of CO_2 absorption were conducted using a laboratory-scale setup, as shown in Figs. 1 and 2, which include an experimental schematic and a photographic picture of the gas injection. The experiment utilizes a pair of Mass Flow Controllers (MFC), one from Brooks® (USA) and the other from Hitachi (Japan): the Model 5851i and the SFC1480FX, respectively used to control and calculate gas mass flow. A stainless-steel diffuser (SFHx, HENGKO, China) with diameters of 0.5, 30, and 500 micrometers to disperse carbon dioxide gas and turn it into bubbles. The diameter of the bubbles depends on the diameter of the diffuser pores. A pressure transmitter (WIKA, Germany) measured the pressure. Also, it was used a dissolved carbon dioxide detector (InPro®5000(i) CO2 Sensors-CO2 Transmitter 5100 e, Mettler-Toledo, USA) integrated with a temperature probe to measure the temperature of the solution. The SINGLE STATION MICRO Plus Controller (760, Foxboro, USA) controlled the operation of the mass flow controller for the carbon dioxide gas exiting from the bubble column. The bubble column was made from a stainless-steel tube of 10 cm (diameter), 40 cm (height) with 3 mm-thick walls. The temperature of the internal solution was regulated by immersing the bubble column in a water bath. The water's temperature was regulated by a temperature

controller of the Hartmann & Braun AG Digitric Z type, while the water bath was cooled by the refrigeration system. The refrigeration system that cooled it consists of a compressor, condenser, evaporator, and capillary tube. The cooling gas was Freon 134. The solution used in the experiment was Reverse Osmosis (RO) water and sucrose in different concentrations.

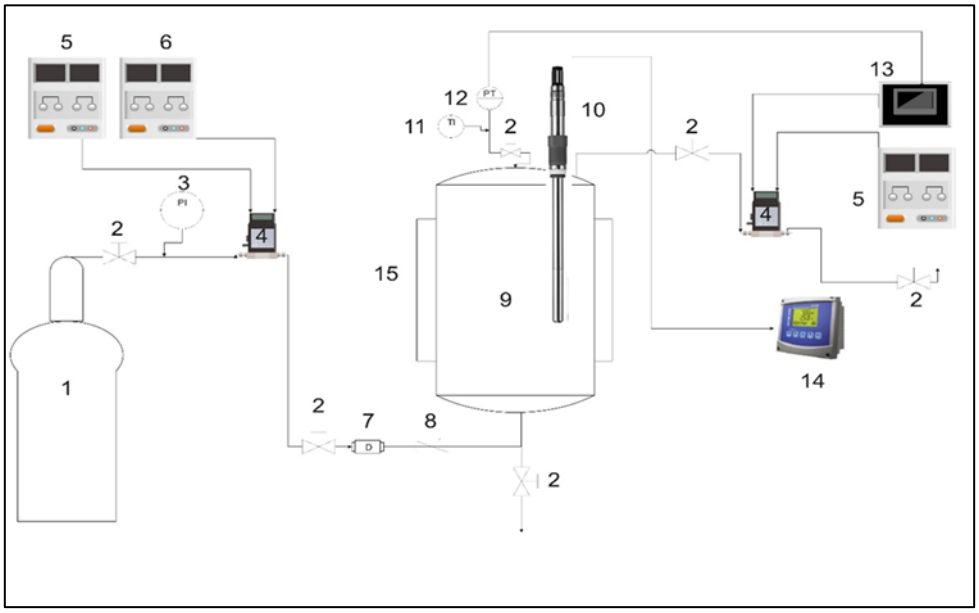

Fig. 1 Experimental Schematic Outline Semi-Batch for CO2 Absorption: (1) CO2 Cylinder, (2) Gate Valves, (3) Pressure Gauge, 4. Mass Flow Controller, 5. Power Supply, 6. Power Supply (Setpoint), 7. Gas Diffuser, 8. Check Valve, 9. Absorber, 10. CO2 Dissolves Probe, 11. Temperature Sensor, 12. Pressure Transmitter, 13. Single-Station Micro Plus Controllers, 14. CO2 Transmitter, and 15. Cooling Water Bath.

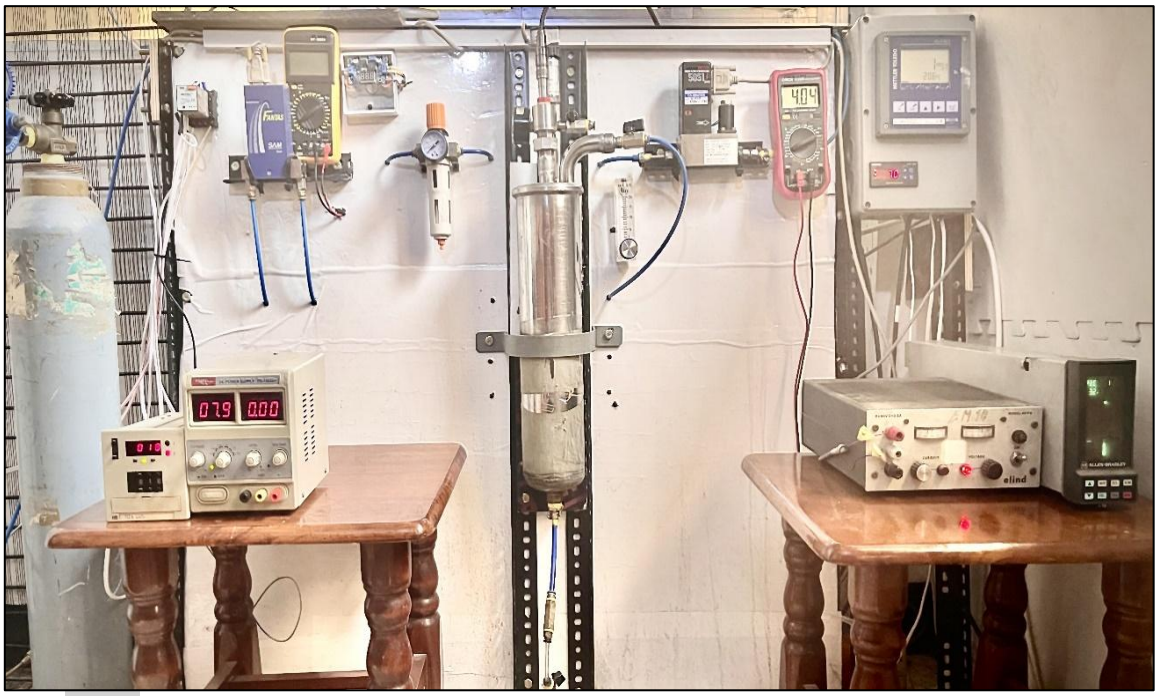

Fig. 2 Photographic Picture of Apparatus Used for Semi-Batch CO_2 Absorption System.

4.2.Experimental Procedure

The experimental procedures are listed below:

1- The solution designated for the experiment was prepared by mixing RO water with different concentrations of sucrose until it was completely dissolved and added to the system.

2- Nitrogen gas was pumped into impurities and concentrations to distribute the solution's temperature.

3- According to the manufacturer's recommendations, MFC must be operated for at least 45 minutes to warm up and stabilize their temperature to ensure measurement accuracy.

4- The cooling system was turned on to reach the desired solution temperature, which was carefully controlled within a tolerance of ± 0.5 degrees Celsius.

5- Carbon dioxide gas flows from a high-pressure cylinder through a pressure regulator to the MFC, controlling the gas flow by weight to maintain consistency even when temperature or pressure changes. The gas then flew through a disperser with micro-diameter pores to achieve smaller bubbles undergoing dissolution in the solution at a constant temperature. Unabsorbed gas flew through the Mass Flow Controller (MFC) to measure the mass flow rate. This procedure continued until the solution reached saturation with CO2 gas.

4.3.Experimental Sets

By using (BBD), the total number of experiments was 45 runs. The D-optimality method was chosen to select the 25 observations that gave the best response. Four variables considered in this study were gas flow rate (L/min), temperature of solution (°C), concentration of sucrose (g/l), and diffuser pore diameter (µm), presented in Table 1. Each variable was varied over three levels.

Table 1 Box–Behnken Experiment Design by Minitab Program.

Description	Variable	Unit	Symbol			
Dependent variable	Yield of CO_2	(%)	Y_{CO2}			
Dependent variable	Volumetric mass transfer coefficient	(1/min)	Kla			
				Range		
Independent Variable (Continues variable)	gas flow rate	(L/min)	Gf	0.2	0.45	0.7
Independent Variable (Categories Variable)	Temperature of solution	(°C)	Ts	5	15	25
	Concertation of Scuros	(g/l)	Cs	0	75	150
	Diffuser pore diameter	(µm)	Df	0.5	30	500

5.RESULTS AND DISCUSSION

The amount of carbon dioxide used in all experiments was equal to 9.75 grams; however, the flow rate was changed at three levels. The first level required 25 minutes to complete and had a flow rate of 0.2 L/min. Similarly, the levels were 0.45 L/min and 0.7 L/min, which required 7 and 11 minutes, respectively.

5.1.Box-Behnken Analysis of the Responses

The results of run experiments are presented in Table 2. The student's t-test evaluates parameter regression coefficient significance. The importance of variable interactions is assessed using P values. Generally, Fischer's 'F test' values with low probability P values suggest significant regression model significance. Larger t and smaller P mean a more significant coefficient term. Table 3 illustrates regression coefficients, t, and P values for linear, quadratic, and interaction effects of all variables Gf, Ts, Cs, and Df on Y_{CO2}.

Table 2 Experimental Design and Response Value for Y_{CO2} and Kla

	Continuous variable			Categories Variable	Responses	
Exp. No.	gas flow rate (L/min)	Temperature (C°)	Concentration of sucrose (g/l)	size of pore diffuser (µm)	Yield $_{CO2}$ (%)	Kla (1/min)
1	0.7	15	0	500	27.77	0.1735
2	0.2	15	150	500	26.48	0.0491
3	0.2	15	0	500	32.25	0.0643
4	0.45	25	150	0.5	29.4	0.4538
5	0.2	5	75	30	45.39	0.0892
6	0.7	15	150	500	26.25	0.1403
7	0.7	5	75	0.5	47.68	0.3984
8	0.45	25	0	30	29.34	0.3066
9	0.2	15	0	0.5	35.67	0.1105
10	0.7	15	150	30	38.02	0.5176
11	0.7	25	75	0.5	29.43	0.6253
12	0.2	25	75	500	24.97	0.0856
13	0.7	5	75	500	31.28	0.1267
14	0.45	5	0	30	47.77	0.2161
15	0.45	5	150	30	49.84	0.3494
16	0.45	25	150	30	29.01	0.5084
17	0.45	15	75	0.5	39.08	0.4291
18	0.2	15	150	0.5	35.77	0.1153
19	0.2	25	75	30	28.36	0.1529
20	0.7	15	0	30	37.46	0.4187
21	0.7	25	75	500	23.13	0.2278
22	0.2	5	75	500	35.06	0.0443
23	0.45	25	0	0.5	29.78	0.451
24	0.45	5	150	0.5	50.58	0.3925
25	0.45	5	0	0.5	51.63	0.2517

The P values indicated that the linear impacts of the experimental variables, specifically Ts and Df, had a statistically significant impact on Y_{CO2} compared to the other two parameters, i.e., Gf and CS. High significance was found for the squared effect of (Gf*Gf) compared to the other factors (Ts, Cs, and DF). The influence of the interaction between the factors was a highly significant effect between (Gf*Df (0.5)), (Ts*Df(0.5)), and (Cs*Df(30)). The p-value for the other interaction variables (Gf*Df(30)), (Ts*Df(30)), and (Cs*Df(0.5)) showed that they insignificantly impacted response.

Table 3 Estimated Regression Coefficients and Corresponding Statistical t- and P-Values for YCO2.

Coded Coefficients for Y_{CO2}					
Term	**Coef.**	**SE Coef.**	**t-Value**	**P-Value**	**VIF**
Constant	36.345	0.428	84.94	0.000	
Gf (L/min)	0.186	0.302	0.62	0.549	1.11
Ts (C°)	-7.916	0.292	-27.15	0.000	1.04
Cs (g/l)	-0.689	0.292	-2.36	0.036	1.04
Df (µm)					
0.5	3.352	0.338	9.92	0.000	1.48
30	2.530	0.338	7.49	0.000	1.39
Gf (L/min)*Gf (L/min)	-2.064	0.557	-3.70	0.003	1.36
Gf (L/min)*Df (µm)					
0.5	1.231	0.448	2.75	0.018	1.83
30	0.246	0.448	0.55	0.592	1.83
Ts (°C) *Df (µm)					
0.5	-2.297	0.397	-5.78	0.000	1.20
30	-1.059	0.397	-2.67	0.021	1.20
Cs (g/l) * Df (µm)					
0.5	0.467	0.397	1.18	0.262	1.20
30	0.666	0.397	1.68	0.120	1.20

5.1.1.The Main Effects and Interaction Plots for (Y_{CO2}) Mains

Figures 3 and 4 illustrate the values of the variables that give the maximum and minimum values for y, together with the impact of the variable interaction on these high and low values. Approximately, the operating conditions of the average gas flow rate, low temperature 5 °C, concentration of scouse (0 g/l), and low diameter of pore diffuser (0.5 µm) gave the highest value for Y_{co2}.

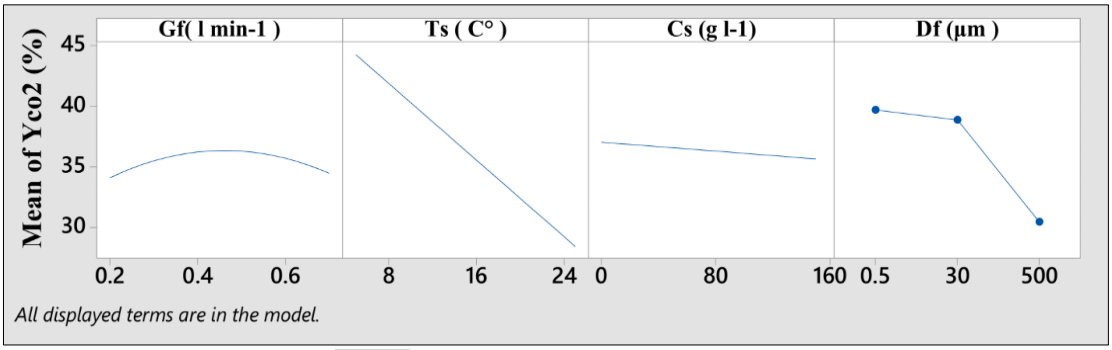

Fig. 3 Main Effects Plots for Y_{CO2}(%).

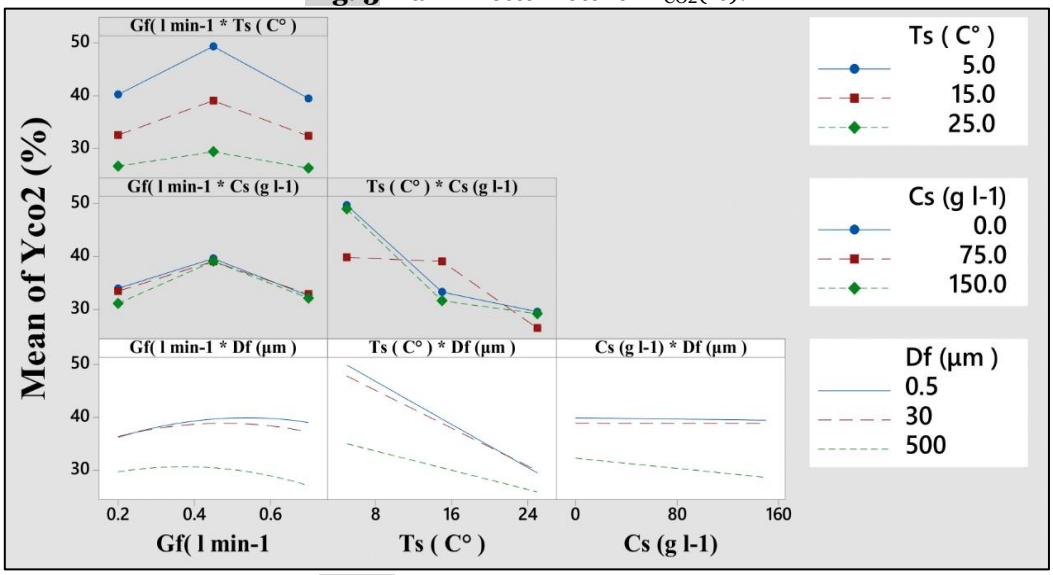

Fig. 4 Interaction Plot for Y_{CO2}(%).

5.1.2.Pareto Chart of the Standardized Effects for Y_{CO2}

The Pareto chart, Fig. 5, compares the significance level of the influence of gas flow rate (Gf), the temperature of the solution (Ts), the concentration of sucrose (Cs), and diffuser pore diameter (Df) on the yield of CO2. On the Pareto chart, bars that cross the reference line are statistically significant. The reference line is at 1.54. The temperature of the solution is more conducive to the yield of CO2. Then, the effect of diffuser pore diameter and the concentration of sucrose on the yield of CO2, respectively. At the same time, the interactive effect of the temperature of the solution and diffuser pore diameter (Ts*DF) interaction had a significantly positive influence. These factors with interaction were statistically significant at the 0.05 level with the present model terms besides the effects of gas flow rate and gas flow rate (Gf*Gf), gas flow rate and diffuser pore diameter (Gf*Df), concentration of sucrose and diffuser pore diameter (Cs*Df). As for the gas flow rate (Gf), it insignificantly impacted YCO2[34].

5.1.3.Residuals Plots for Yield Analysis

From Fig. 6, it is clear that the residuals were distributed normally. The drawings can judge them, as the values in a Normal probability plot form a large number of points very close to the line, and in fitted value form, the points do not have a defined shape scattered randomly. In the histogram, there is a vertex representing a data set with one mode, which is unimodal. In the form of an observation order, there are no red points, i.e., the data distributed within the range. In conclusion, the plots in Fig. 6 show that the model accurately described the carbon dioxide (Y_{CO2}) absorption yield. The results of run experiments are presented in Table 2. The student's t-test evaluates parameter regression coefficient significance. The importance of variable interactions is assessed using P values. Generally, Fischer's 'F test' values with low probability P values suggest significant regression model significance. Larger t and smaller P mean a more significant coefficient term. Table 4 illustrates regression coefficients, t, and P values for linear, quadratic, and interaction effects of Gf, ts, Ts, and Df on Kla.

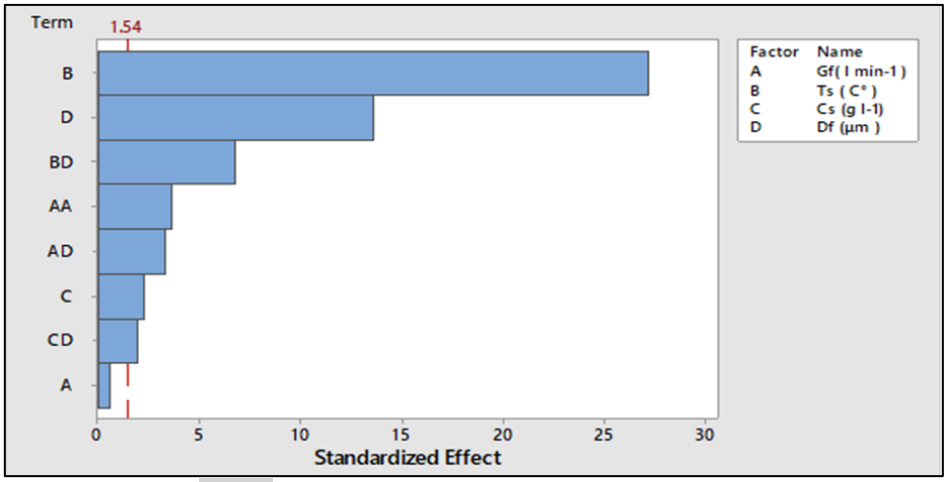

Fig. 5 Pareto Chart of the Standardized Effect.

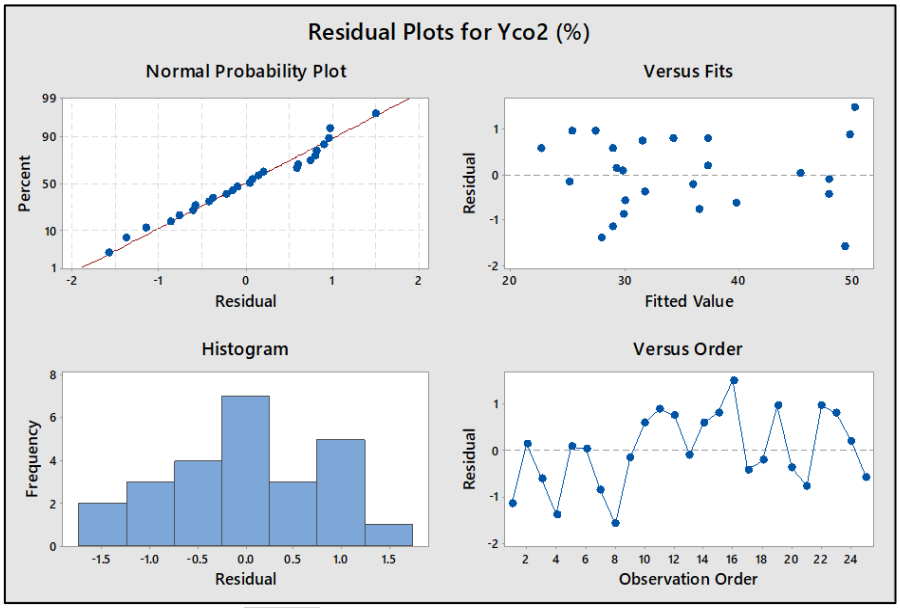

Fig. 6 Residual Plots for Yco2 (%).

Table 4 Estimated Regression Coefficients and Corresponding Statistical t- and P-Values for Kla.

Coded coefficients for Kla					
Term	**Coef.**	**SE Coef.**	**t-Value**	**P-Value**	**VIF**
Constant	0.3081	0.0133	23.1	0.000	
Gf (L/min)	0.14205	0.00941	15.1	0.000	1.11
Ts (C°)	0.05894	0.00892	6.61	0.000	1
Cs (g/l)	0.02832	0.00909	3.12	0.008	1.04
Df (µm)					
0.5	0.0807	0.0105	7.66	0.000	1.48
30	0.0457	0.0105	4.34	0.001	1.39
Gf (L/min)*GF (L/min)	-0.0677	0.0174	-3.9	0.002	1.36
GF (L/min)*Ts (C°)	0.0279	0.0126	2.21	0.046	1
GF (L/min)*Df (µm)					
0.5	0.0574	0.014	4.12	0.001	1.83
30	0.0315	0.014	2.26	0.042	1.83
Cs (g/l) *Df (µm)					
0.5	-0.0036	0.0124	-0.29	0.777	1.2
30	0.044	0.0124	3.55	0.004	1.2

5.1.4.The Main Effects and Interaction Plots for (Kla) Mains

Figures 7 - 8 illustrate the values of the variables that give the maximum and minimum values for y, together with the impact of the variable interaction on these high and low values. Approximately, the average value of the gas flow rate, low temperature 25 °C, concentration of scouse (150 g/l), and low diameter of pore diffuser (0.5 µm) gave the highest value for Y_{CO_2}.

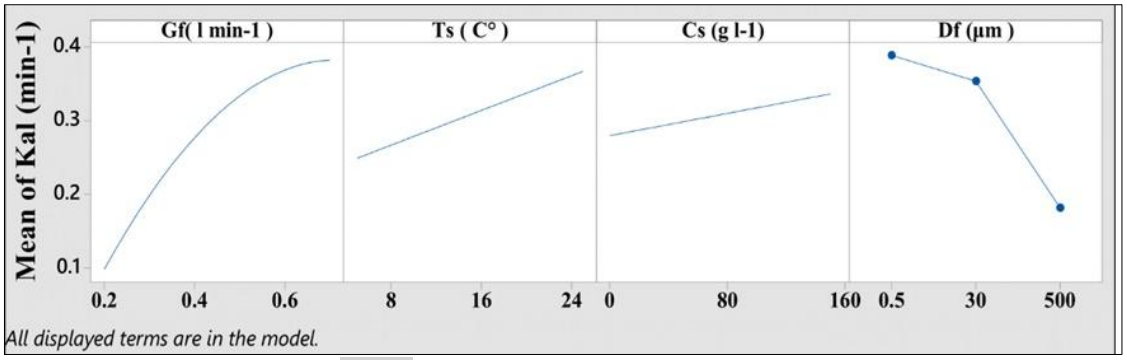

Fig. 7 Main effects plots for kla min^{-1}.

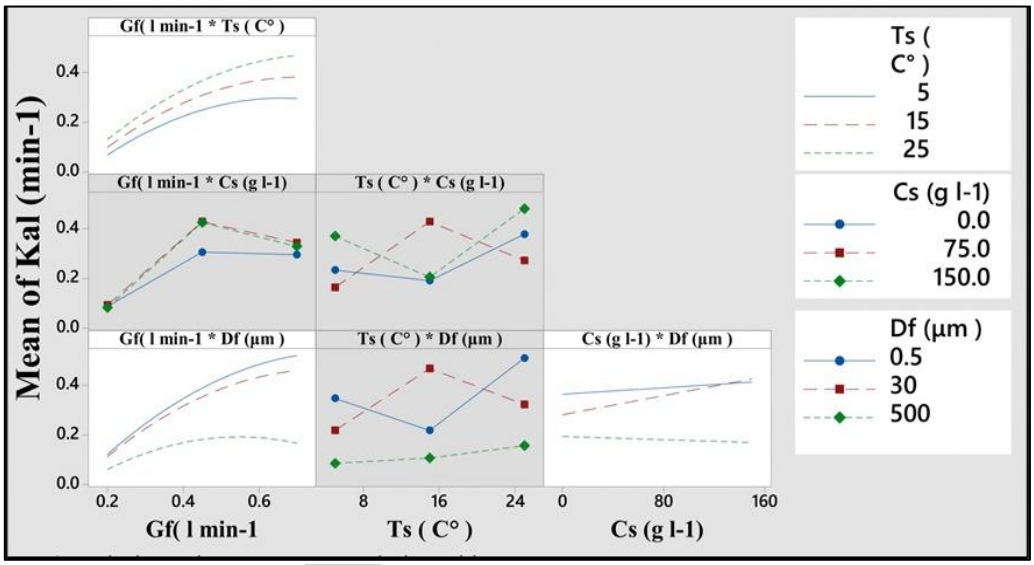

Fig. 8 Interaction Plot for kla min^{-1}.

5.1.5.Pareto Chart of the Standardized Effects for Kla

The Pareto chart in Fig. 9 compares the significance level of the influence of gas flow rate (Gf), the temperature of the solution (Ts), the concentration of sucrose (Cs), and diffuser pore diameter (Df) on the yield of CO2. On the Pareto chart, bars that cross the reference line are statistically significant. The reference line is at 1.53, at the 0.05 level with the present model terms. The gas flow rate was more conducive to the Kla than the effects of diffuser pore diameter, the temperature of the solution, and the concentration of sucrose on the Kla. At the

same time, the interactive effects of gas flow rate and diffuser pore diameter (Gf*DF) interaction had a significantly positive influence besides the effects of both gas flow rate and gas flow rate (Gf*Gf), concentration of sucrose and diffuser pore diameter (Cs*Df), gas flow rate and temperature of solution (Gf*Ts) [34].

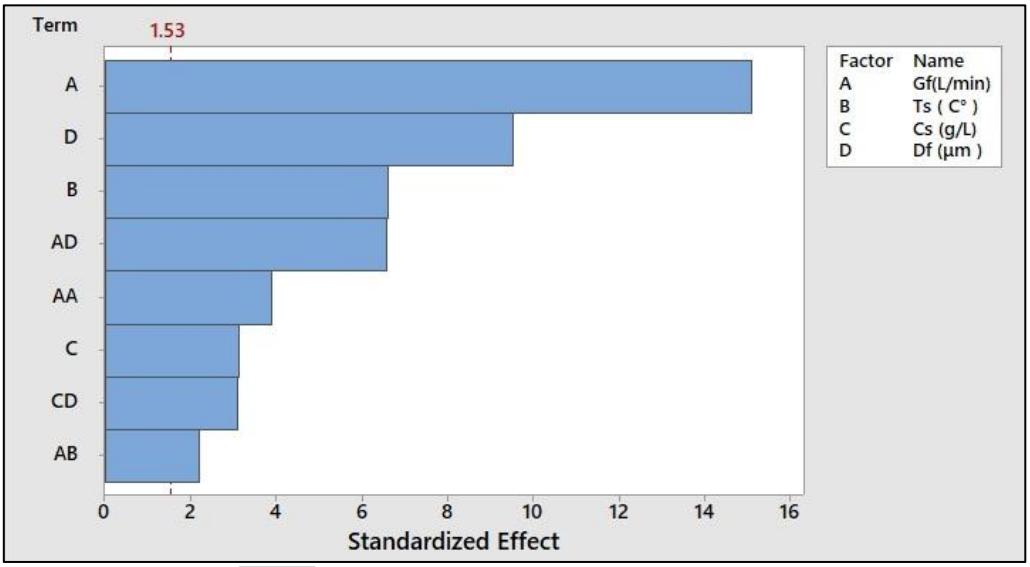

Fig. 9 Pareto Chart of the Standardized Effect.

5.1.6.Residuals plots for Kal analysis

Figure 10 illustrates that all residuals fell from -0.05 to +0.05. They are randomly distributed about zero, suggesting a high correlation between the observed and anticipated values. The analysis of residuals showed no evidence of outliers, as all residuals fell within this range [35].

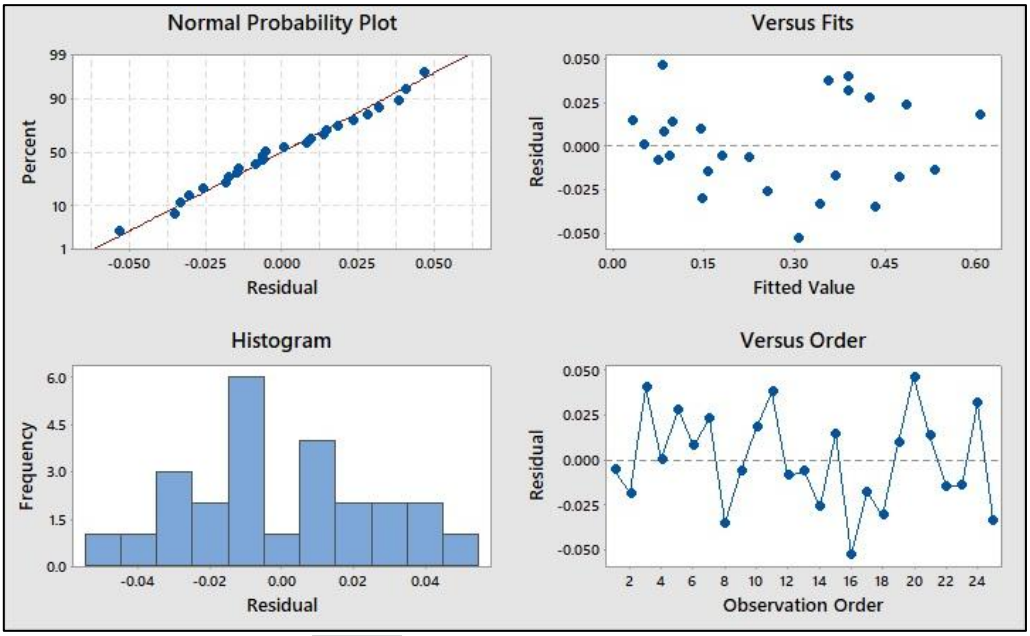

Fig. 10 Residual Plots for Kla (%).

5.1.7.Analysis of Variance (ANOVA)

The statistical significance of the ratio between the mean square variation attributed to regression and the mean square residual error was assessed by analyzing variance (ANOVA). It is a strategy for statistical hypothesis testing in which the overall variation in a data set is divided into pieces linked with distinct sources of variation. In Table 6, ANOVA shows higher F values for all regressions. A large F value suggests that the regression equation explains most of the response variation. The p-value estimates whether F is statistically significant. The observed P values in Table 6 for all the regression analyses were less than 0.01, implying a significant correlation between the response variable and at least one of the factors in the regression equation. The F value of 113.53 in the ANOVA for Y_{CO_2} indicated a substantial effect of the model terms on the response. The model produced R^2 99.13% and adjusted R^2 98.25%, i.e., the proposed model cannot explain at least 0.87 % of experimental outcomes. A chance of $p < 0.05$ exists. At 95%

probability, the model terms were significant. Factors or interactions with p < 0.05 were significant. R^2 = 95.92, as predicted, indicates that the present model has a significant block effect. A value of (predicted R^2 –adjusted R^2) <±0.20 indicates no problem with the data or the model. Similarly, the ANOVA analysis revealed that the F value of 50.26 for Kal showed a significant impact of the model terms on the response variable. The model yields an R-squared value of 97.7% and an adjusted R-squared value of 95.76%, implying that the proposed model was unable to account for a minimum of 2.3 % of observed experimental results. There was a probability of p < 0.05. The model terms exhibited significance at a confidence level of 95%. Significant factors or interactions are those with a p-value less than 0.05. The obtained R^2 value of 91.62% aligns with the predicted outcome, proving that the present model exhibited a substantial block effect. A discrepancy of (predicted R^2 – adjusted R^2) within the range of < ±0.20 suggests that there is either no problem with the data or the model [36, 37]. Using the results of the analysis of variance (ANOVA), the following second-order polynomial equations can be derived to represent the YCO_2 and Kla models: (6, 7, 8, 9, 10, and 11) in terms of experimental variables (with a confidence level of 95% or higher).

Table 6 Analysis of Variance Model Regression for Y_{CO_2} and Kla.

Source	DF		Adj SS		Adj MS		F		P	
	Y_{CO_2}	Kla	Y_{CO_2}	Kla	Y_{CO_2}	Kla	Y_{CO_2}	Kla	Y_{CO_2}	Kla
Regression	12	11	1787.32	0.704331	148.944	0.064030	113.58	50.26	0.000	0.000
Linear	5	5	1288.94	0.507401	257.788	0.101480	196.57	79.66	0.000	0.000
Square	1	1	17.99	0.019378	17.988	0.019378	13.72	15.21	0.003	0.002
Interaction	6	5	111	0.096556	18.501	0.019311	14.11	15.16	0.000	0.000
Error	12	13	15.74	0.016561	1.311	0.001274				
Total	24	24	1803.06	0.720892						
	Yco2		**Kla**							
R^2	99.13		97.7							
R^2 adjusted	98.25		95.76							
R^2 predicted	95.92		91.62							

Df (µm)

0.5 Y_{CO_2} (%) = **46.00 + 35.39 Gf - 1.0213 Ts - 0.00296 Cs - 33.03 Gf*Gf** (6)

30 Y_{CO_2} (%) = **44.90 + 31.45 Gf- 0.8975 - 0.00031 Cs - 33.03 Gf*Gf** (7)

500 Y_{CO_2} (%) = **34.76 + 24.56 Gf- 0.4560 Ts - 0.02430 Cs - 33.03 Gf*Gf** (8)

Df (µm)

0.5 **Kla (L/min) = -0.2277 + 1.606 Gf+ 0.00088 Ts + 0.000330 Cs - 1.084 Gf*Gf+ 0.01115 Gf*Ts** (9)

30 **Kla (L/min) = -0.2636 + 1.502 Gf + 0.00088 Ts + 0.000964 Cs - 1.084 Gf*Gf + 0.01115 Gf*Ts** (10)

500 **Kla (L/min) = -0.1345 + 1.021 Gf + 0.00088 Ts - 0.000161 Cs - 1.084 Gf*Gf + 0.01115 Gf*Ts** (11)

5.1.8.Process Optimization

High carbon dioxide yield (YCO2) and mass transfer coefficient (KLa) are necessary for efficient CO2 absorption when using a sweetener solution for various purposes. This study aims to identify the optimum conditions for maximizing the YCO2 and KLa of CO2 in a sucrose solution. Utilizing a response surface methodology (RSM) with a Box-Behnken design (BBD) facilitated this goal. Numerical optimization using the desirability function was used to choose the optimal values for different operating parameters, such as temperature, sucrose concentration, gas flow rate, and pore diffuser diameter. The optimal obtained response for maximum (YCO2) was 50.37 %. The operational conditions were as follows: pore size of diffuser (0.5 µm), gas flow rate (0.534 L/min), temperature of absorbent (5 °C), and sucrose concentration (0 g/l). The optimal obtained responses for maximum (kla) were 0.632 1/min. The operational conditions were as follows: pore size of the diffuser (0.5 µm), gas flow rate (0.7 L/min), temperature of absorbent (25 °C), and sucrose concentration (150 g/l). The optimal responses obtained for maximum (YCO2 and Kla) were 49.2 % and 0.455 1/min, respectively. The operational conditions were as follows: pore size of the diffuser (0.5 µm), gas flow rate (0.68 L/min), the temperature of absorbent (5 °C), and sucrose concentration (150 g/l) [38].

5.2.Effect of Operating Parameters on CO2 Absorption YCO2

5.2.1.Effect of CO_2 Gas Flow Rate

Figure 11 shows the relationship between the flow rate of CO_2 gas in L/min and the yield of CO_2 absorption (Y_{CO_2}). The graph demonstrates an upward trend in yield as the gas flow rate increases, ranging from 0.2 to 0.6 L/min. Subsequently, the yield of CO_2 absorption experiences a drop, eventually reaching a rate of 0.7 L/min. This decrease can be attributed to the duration required for the gas bubbles to pass through the bubble column, a period influenced by the velocity of the gas bubble flow. Furthermore, the presented figure illustrates an inverse relationship between the size of the diffuser pores and the yield. This relationship indicates that the yield increased as the size of the diffuser pores decreased. This result can be attributed to producing smaller and more numerous bubbles, consequently enhancing the surface area of contact between

the gas and the liquid. A rise in the flow rate of carbon dioxide from 0.2 to 0.6 L/min resulted in the following outcomes: In the instances of pore size diffuser 0.5µm, 30 µm, and 500 µm, the yield exhibited increasing. Specifically, for 0.5 µm, the yield rose from 46.25% to 50.03%. Similarly, for 30 µm diffuser, the efficiency climbed from 45.15% to 47.93%. Lastly, in the case of 500 µm diffuser, the yield experienced an increase from 34.24% to 35.3%. These results were consistent with studies on carbon dioxide absorption [39].

5.2.2.Effect of Temperature

Figure 12 shows that for all types of gas diffusers. Y_{CO2} decreased significantly when the absorbent temperature increased. These decreases can be explained by elevated temperatures leading to a corresponding augmentation in kinetic energy. The increased kinetic energy of gas molecules resulted in enhanced molecular motion and a reduction in intermolecular cohesive forces, causing a drop in surface tension, leading to the disruption of intermolecular bonds and subsequent escape from the solution. The solubility of gases in water has an inverse relationship with temperature. Therefore, it enables the escape of gas molecules absorbed into the liquid. The maximum CO_2 yield was (49.81%) at a temperature of 5°C while employing a gas dispersion mechanism with a pore diameter of 0.5 µm. The observed percentage experienced a significant reduction. It dropped by nearly half (24.63%) as the temperature rose to 25 °C. A larger pore diameter of 500 µm was employed. These results were consistent with studies on carbon dioxide absorption [40-42].

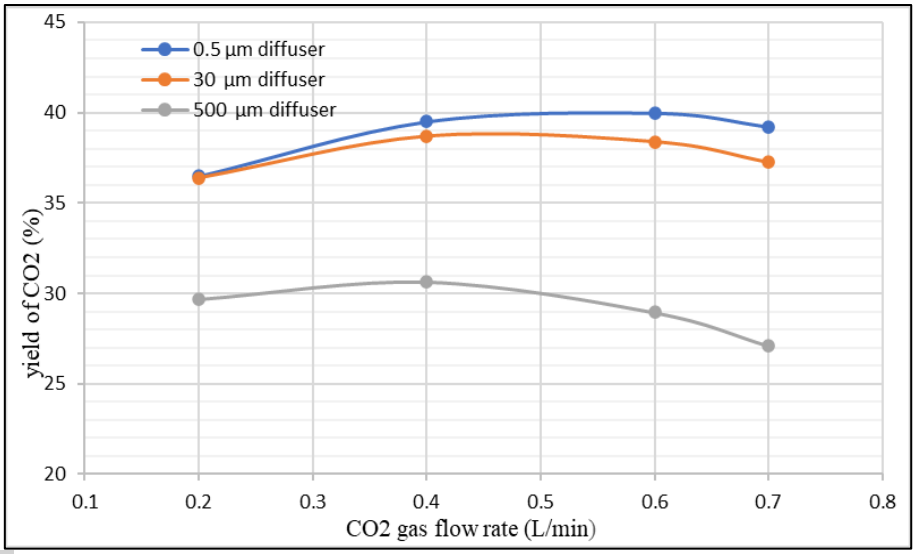

Fig. 11 Effect of Gas Flow Rate on the Yield of Carbon Dioxide at T = 15 °C, P = 1 atm, and Concentration of Sucrose = 75 g/l with different Sizes of Gas Diffuser.

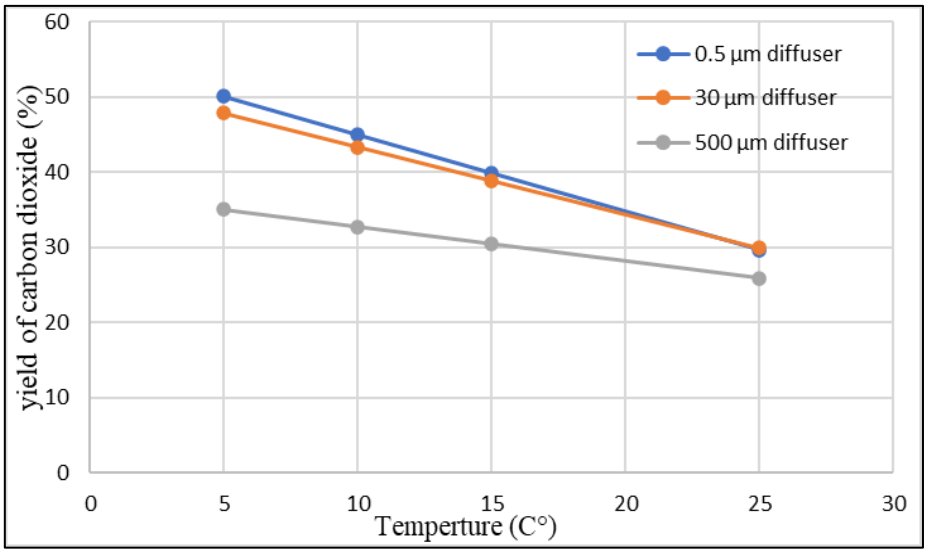

Fig. 12 Effect of Temperature on the Yield of Carbon Dioxide at Gas Flow Rate = 0.45 L/min, p = 1 atm, and Concentration of Sucrose = 75 g/l.

5.2.3.Effect of Sucrose Concentration

Figure 13 illustrates the impact of varying sugar concentrations on the experiment results. It is evident that the influence of sugar concentration on the absorption yield of CO_2 was small. Specifically, the CO_2 yield declined from 50.25% to 49.81% at a sucrose concentration of 0 to 150 g/l when employing a gas dispersion system with a pore diameter of 0.5 µm. The observed drop in concentration between the two measurements was 0.8% from the initial value. Similarly, when utilizing diffusers with pore diameters of (30 µm and 500 µm), the proportion of CO_2 yield decreased from (48.31% and 37.12%) to (47.55% and 34.48%); both yields decreased by (1.65%) and (9.7%), respectively. The decrease in carbon dioxide gas absorption with increasing sugar concentration is due to changes in the physical properties of the solution, including increased density, viscosity, and surface tension, as well as decreased diffusivity. The modifications resulted in a reduction in the rate at which CO2 was absorbed. According to Fig. 15, it can be concluded that the influence of sugar concentration increased with the diameter of the pores in the gas diffuser. These results are consistent with studies on carbon dioxide absorption [41].

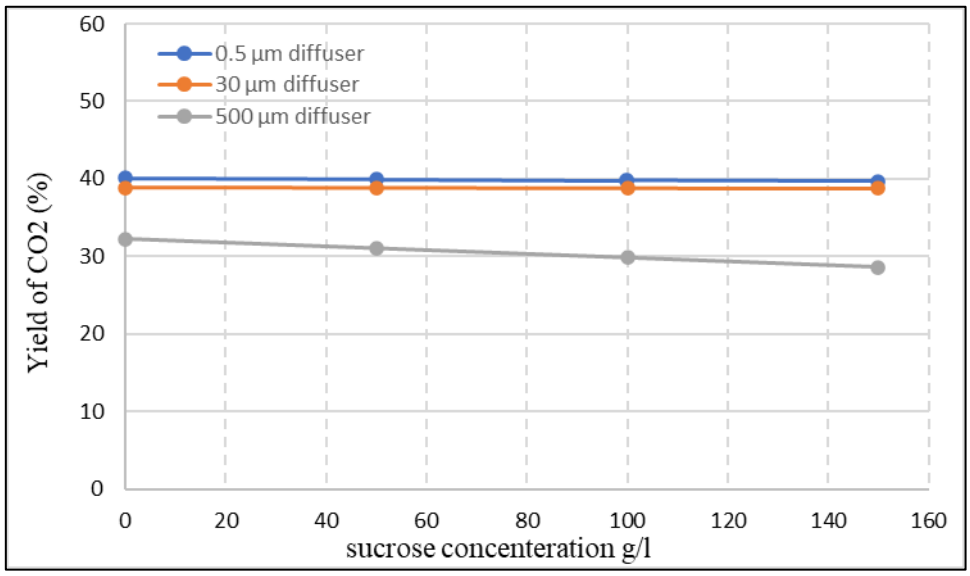

Fig. 13 Effect of Sucrose Concentration on the Yield of Carbon Dioxide at T = 15 °C, p = 1 atm, and Gas Flow Rate = 0.45 L/min.

5.3.Effect of Operating Parameters on Volumetric Mass Transfer Coefficient (Kla)

5.3.1.Effect of CO_2 Gas Flow Rate

Figure. 14 illustrates the correlation between the quantity of gas flow rate and the volumetric mass transfer coefficient. It has been observed that the volumetric mass transfer coefficient (Kla) increased with the gas flow rate. This behavior is consistent across various pore-size diffusers. Furthermore, a non-linear relationship between Kla and the gas flow rate was identified, indicating a clear dependency of the volumetric mass transfer coefficient on the gas flow rate. The diagram also elucidates that when the pore size was reduced, there was an increase in the volumetric mass transfer coefficient. It is common knowledge that an increase in the flow rate of gas increases the mass transfer coefficient because increasing flow rate results in an increased amount of new fluid elements entering the mass transfer contact. If more fluid elements are introduced to the interface, the mass transfer driving force will increase, which will, in turn, cause the molar flux to increase to a greater degree. Additionally, more eddies will be produced. The Kla was observed to be (0.52 L/min) at a gas flow rate of (0.7 L/min) and (0.12 L/min) at a gas flow rate of (0.2 L/min) while employing a gas dispersion mechanism with a pore diameter of 0.5 µm. In the same context, the Kla was observed to be (0.46 1/min) and (0.19 1/min) at gas flow rates of (0.7 L/min), (0.11 1/min) and (0.085 1/min) at a gas flow rate of 0.2 L/min. This investigation depends on using a pore diffuser with a diameter of 30 and 500 µm, respectively. These results were consistent with studies on carbon dioxide absorption and volumetric mass transfer coefficient [22, 36, 43, 44].

5.3.2.Effect of Temperature

Figure 15 illustrates that the volumetric mass transfer coefficient (Kla) experienced a substantial increase across all gas diffuser types when the absorbent temperature increased. The solubility of carbon dioxide was influenced by changes in temperature. Elevated temperatures were observed to induce a reduction in the solubility of carbon dioxide (CO_2), diminishing the driving force and subsequently decreasing the rate of CO_2 absorption. Nevertheless, it is worth noting that the diffusion rate for carbon dioxide (CO_2) had

an upward trend as temperatures increased, accompanied by a simultaneous drop in both liquid viscosity and g/l surface tension. Consequently, these factors lead to an augmented Kla value. The potential benefits resulting from the rise in temperature on Kla may counterbalance the diminished driving power attributed to reduced CO_2 solubility. Elevated temperatures have been observed to result in increased mass transfer coefficients. However, it should be noted that the mutual solubility of phases generally increased with temperature, hence exerting a detrimental effect on subsequent separation processes. At a solution temperature of 5°C, Kla was (0.33 1/min); at 25 °C, it was (0.44 1/min) when using a gas diffuser with a pore diameter of 0.5 µm. In the same situation, the Kla was (0.29 1/min) and (0.14 1/min) at a solution temperature of 5 °C, (0.41 1/min), and (0.26 1/min) at 25 °C for the other diffuser with a 30 and 500 µm pore size diameter, respectively. These results were consistent with studies on carbon dioxide absorption and volumetric mass transfer coefficient [22].

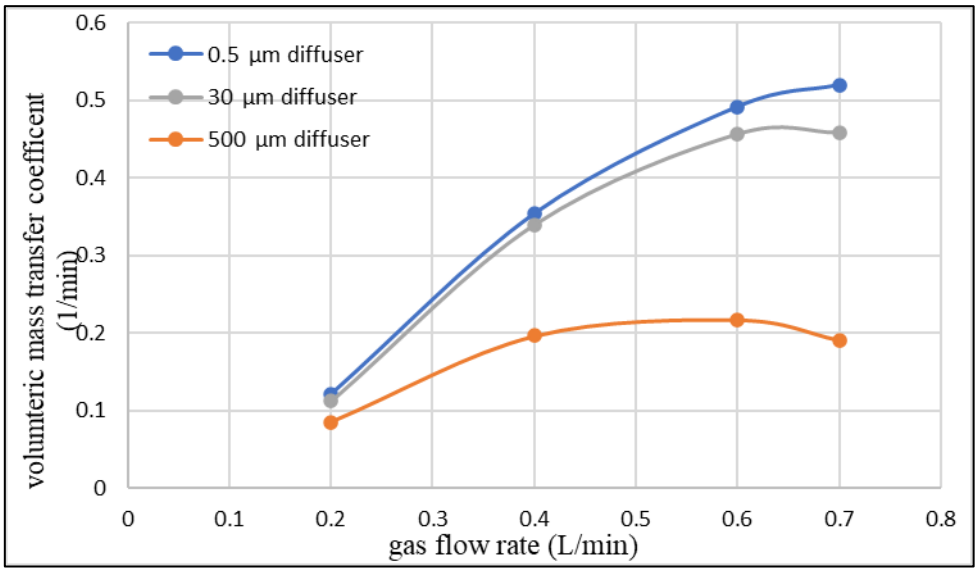

Fig. 14 Effect of Gas Flow Rate on the Volumetric Mass Transfer Coefficient of Carbon Dioxide at T = 15 °C, p = 1 atm, and Concentration of Sucrose = 75 g/l.

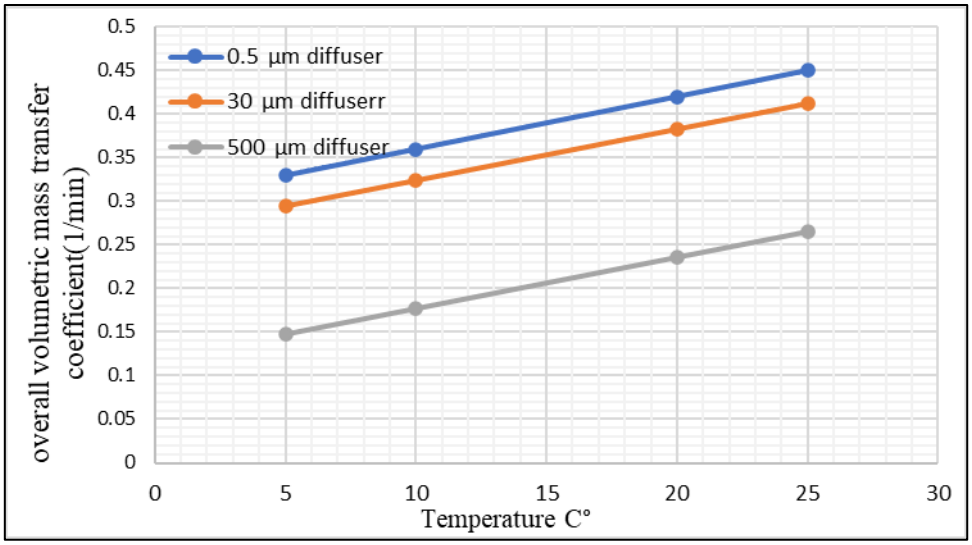

Fig. 15 Effect of Temperature on the Volumetric Mass Transfer Coefficient of Carbon Dioxide at Gas Flow Rate = 0.45 L/min, p = 1 atm, and Concentration of Sucrose = 75 g/l.

5.3.3.Effect of Sucrose Concentration

Figure 16 shows the effect of the sucrose concentration of the solution on the volumetric mass transfer coefficient. The volumetric mass transfer coefficient (Kla) increased with sucrose concentration. At (150 g/l) sucrose concentration, the Kla was (0.1/min), while for pure water, it was (0.36 1/min) when using a gas diffuser with a pore diameter of 0.5 µm. In the same situation, the Kla was (0.42 1/min) and (0.25 1/min) at a sucrose concentration of the solution was (150 g/l), and (0.28 1/min) and (0.19 1/min) when the solution of pure water for the other diffuser with a 30 and 500 µm pore size diameter, respectively. These results are consistent with studies on carbon dioxide absorption and volumetric mass transfer coefficient [36].

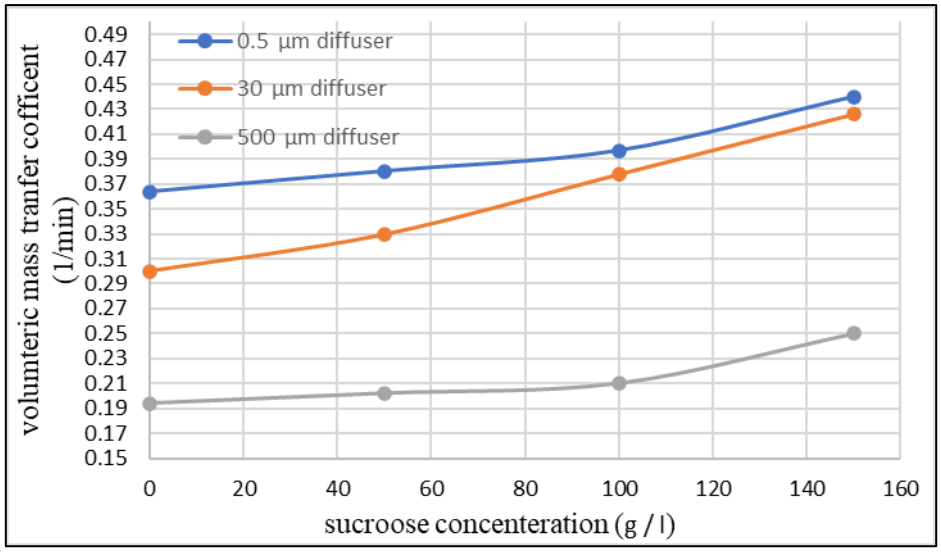

Fig. 16 Effect of Sucrose Concentration on the Volumetric Mass Transfer Coefficient of Carbon Dioxide at T = 15 °C, p = 1 atm, and Gas Flow Rate = 0.45 L/min.

6.CONCLUSION

In this study, the effect of operating conditions and the concentration of sucrose in pure water under atmospheric pressure on the amount of carbon dioxide dissolved in the solution was studied. Also, the volumetric mass transfer coefficient was practically studied. Three gas dispersions with different pore diameters were investigated. The relationship between the gas flow rate and the yield of CO_2 exhibited an exponential connection until a flow rate of (0.45 L/min), beyond which it transitioned to an inverse relationship until (0.7 L/min). Regarding its correlation with temperature, there was an inverse association across all diffusers. Moreover, the impact of sucrose content was found to be minimal and nearly imperceptible. All correlations with the volumetric mass transfer rate were found to be expulsions. Furthermore, an inverse relationship existed between the diameter of the diffuser pores and their effect. Box Behnken analysis given a regression equation with R^2 =99.13 %, adjusted R^2 =98.25%, and predicted R^2 =95.92%, similarly, R^2 =97.7 % adjusted R^2 =95.76%, and predicted R^2 =91.62% for Kal response. The F-test and P values were used to determine which experimental factors have a significant impact, according to the P values for the linear and squared effects of experimental variables on responses. All variables and interactions had a high significance on the responses. The optimization operation conditions for maximum Y_{CO_2} (50.37%) were (Gf = 0.5342 L/min), (Ts = 5 °C), Cs = 0 g/l), and Df = (0.5 µm). The optimization operation conditions for maximum Kla (0.632 1/min) were (Gf = 0.7 L/min), (Ts = 25°C), Cs = (150 g/l), and Df = (0.5 µm). The optimization operations conditions for maximum Y_{CO_2} and kla (49.2 % and 0.455 1/min) were (Gf = 0.68 L/min), (Ts = 5 °C), (Cs =150 g/l), and (Df = 0.5 µm), respectively.

ACKNOWLEDGEMENTS

The authors thank the employees of the Ministry of Industry and Minerals - Mansur factory for their invaluable assistance and resources in making this research possible, as well as the Chemical Engineering Department, College of Engineering, Baghdad University. University order No: D4/2818 on 9/4/2020.

NOMENCLATURE

Symbol	Description	Unit
a	interfacial area	m^2/m^3
a_o	regression equation constant	
a_{ii} , a_{ij}	regression coefficients of the model	
ANOVA	Analysis of variance	
BBD	Box-Behnken design	
C	CO2 Concertation	
Cs	Concertation of Sucrose	g/l
Df	pore size diameter	µm
Gf	gas flow rate	L/min
Kla	volumetric mass transfer coefficients	1/min
KOL	overall mass transfer coefficient of liquid phases	
KOV	overall mass transfer coefficient of vapor phases	
MEA	mono ethanol amine solution	
MFC	Mass Flow Controllers	
n	number of mole	mole
Nv	rate of mass transfer in the liquid phase per unit volume	mole/s .m^3
R^2	Coefficient of Determination	
RSM	response surface methodology	
t	time	min
Ts	Temperature of solution	℃
Ui	real value of the independent variable	
Uo	real value of the independent variable at the center point	
X	independent variable	
YCO2	carbon dioxide absorption yield	%
ΔUi	step change value	
$Wt_{CO_2\ absorb}$	amount of CO2 dissolved	g
$Wt_{CO_2\ total}$	Total amount of CO2	g
Subscripts		
*	Saturation	
L	solute-dissolved	

REFERENCES

[1] Kregiel D. **Health Safety of Soft Drinks: Contents, Containers, and Microorganisms.** *BioMed Research International* 2015; **2015**: 1–15.

[2] Kraakman NJR, Rocha-Rios J, van Loosdrecht MCM. **Review of mass transfer aspects for biological gas treatment.** *Applied Microbiology and Biotechnology* 2011; **91**(4): 873–886.

[3] Elhajj J, Al-Hindi M, Azizi F. **Review of the Absorption and Desorption Processes of Carbon Dioxide in Water Systems.** *Industrial and Engineering Chemistry Research* 2013; **53**(1): 2–22.

[4] Sieblist C, Jenzsch M, Pohlscheidt M. **Influence of Pluronic F68 on Oxygen Mass Transfer.** *Biotechnology Progress* 2013; **29**(5): 1278–1288.

[5] Danckwerts PV. **Significance of Liquid-Film Coefficients in Gas Absorption.** *Industrial and Engineering Chemistry* 1951; **43**(6): 1460–1467.

[6] Van Elk EP, Knaap MC, Versteeg GF. **Application of the Penetration Theory for Gas–Liquid Mass Transfer without Liquid Bulk: Differences with Systems with a Bulk.** *Chemical Engineering Research and Design* 2007; **85**(4): 516–524.

[7] Wang C, Xu Z, Lai C, Sun X. **Beyond the Standard Two-Film Theory: Computational Fluid Dynamics Simulations for Carbon Dioxide Capture in a Wetted Wall Column.** *Chemical Engineering Science* 2018; **184**: 103-110.

[8] Abe S, Okawa H, Hosokawa S, Tomiyama A. **Dissolution of a Carbon Dioxide Bubble in a Vertical Pipe.** *Journal of Fluid Science and Technology* 2008; **3**(5): 667–677.

[9] Yan X, Zheng K, Su W, Wang L, Zhang H, Cao Y, et al. **Predictions of Terminal Rising Velocity, Shape and Drag Coefficient for Particle-Laden Bubbles.** *Minerals Engineering* 2021; **173**: 107188.

[10] Al-mashhadani MKH, Wilkinson SJ, Zimmerman WB. **Carbon Dioxide Rich Microbubble Acceleration of Biogas Production in Anaerobic Digestion.** *Chemical Engineering Science* 2016; **156**: 24–35.

[11] Maceiras R, Nóvoa XR, Álvarez E, Cancela MA. **Local Mass Transfer Measurements in a Bubble Column using an Electrochemical Technique.** *Chemical Engineering and Processing - Process Intensification* 2007; **46**(10): 1006–1011.

[12] Mahmood RS, Alsarayreh AA, Abbas AS. **Measurement and Analysis of Bubble Size Distribution in the Electrochemical Stirred Tank Reactor.** *Iraqi Journal of Chemical and Petroleum Engineering* 2023; **24**(1): 27–31.

[13] Bao Y, Jia J, Tong S, Gao Z, Cai Z. **Review on Single Bubble Gas–Liquid Mass Transfer.** *Chinese Journal of Chemical Engineering* 2020; **28**(11): 2707–2722.

[14] Waisi BI, Majeed JT, Majeed NS. **Carbon Dioxide Capture using Nonwoven Activated Carbon Nanofiber.** *IOP Conference Series: Earth and Environmental Science* 2021; **779**(1): 012056.

[15] Majeed NS, Majeed JT. **Study the Performance of Nanozeolite NaA on CO2 Gas Uptake.** *Iraqi Journal of Chemical and Petroleum Engineering* 2017; **18**(2): 57–67.

[16] Dhuyool AW, Shakir IK. **Carbon Dioxide Capturing via a Randomly Packed Bed Scrubber using Primary and Poly Amine Absorbents.** *Journal of Ecological Engineering* 2023; **24**(11): 14–29.

[17] Al-Hemiri A, Selman MD. **Estimation of Mass Transfer Coefficents in a Packed Distillation Column using Batch Mode.** *Iraqi Journal of Chemical and Petroleum Engineering* 2011; **12**(1): 13–21.

[18] Jaber SF, Abdul wahab YM, Zboon SM. **Investigation of Factors Affecting the Efficiency of Carbon Dioxide Removal in a Single Perforated Sieve Tray Column.** *Journal of Petroleum Research and Studies* 2021; **2**(2): 35–43.

[19] Al-Hemiri AA, Salih SA. **Prediction of Mass Transfer Coefficient in Bubble Column using Artificial Neural Network.** *Journal of Engineering* 2007; **13**: 1-15.

[20] Chen PC, Huang CH, Su T, Chen HW, Yang MW, Tsao JM. **Optimum Conditions for the Capture of Carbon Dioxide with a Bubble-Column Scrubber.** *International Journal of Greenhouse Gas Control* 2015; **35**: 47–55.

[21] Liu Q, Endo H, Fukuda K, Shibahara M, Zhang P. **Experimental Study on Solution and Diffusion Process of Single Carbon Dioxide Bubble in Seawater.** *Mechanical Engineering Journal* 2016; **3**(5): 16–00269.

[22] Al-Hindi M, Azizi F. **The Effect of Water Type on the Absorption and Desorption of Carbon Dioxide in Bubble Columns.** *Chemical Engineering Communications* 2019; **207**(3): 339–349.

[23] Inkeri E, Tynjälä T. **Modeling of CO2 Capture with Water Bubble Column Reactor.** *Energies* 2020; **13**(21): 5793.

[24] Xu X, Kordorwu V, Li Z, Liu F, Wei W, Liu Z. **Experimental Study on the Dynamics and Mass Transfer of CO2 Bubbles Rising in Viscoelastic Fluids.** *International Journal of Multiphase Flow* 2021; **135**: 103539.

[25] Sa'adiyah DS, Matsuo Y, Schlüter M, Kurimoto R, Hayashi K, Tomiyama A. **Effects of Chemical Absorption on Mass Transfer from Single Carbon Dioxide Bubbles in Aqueous Sodium Hydroxide Solution in a Vertical Pipe.** *Chemical Engineering Science* 2021; **245**: 116852.

[26] Nock WJ, Heaven S, Banks JK. **Mass Transfer and Gas–Liquid Interface Properties of Single CO2 Bubbles Rising in Tap Water.** *Chemical Engineering Science* 2016; **140**: 171–178.

[27] Najim SE, Ateik AA, Haweel CK. **Effect of Operating Conditions on CO2 Absorption into Aqueous Alkanol Amine Solutions in Packed Column.** *University of Thi-Qar Journal for Engineering Sciences* 2011; **2**(1): 103-117.

[28] Atiya ZY. **Estimation of Volumetric Mass Transfer Coefficient in Bioreactor.** *Al-Khwarizmi Engineering Journal* 2012; **8**(3): 75-80.

[29] Gul A, Unut U. **Carbon Dioxide Absorption Using Different Solvents (MEA, NaOH, KOH and Mg (OH) 2) in Bubble Column Reactor.** *Bitlis Eren Üniversitesi Fen Bilimleri Dergisi* 2023; **12**(2): 418-427.

[30] Atzori F, Barzagli F, Varone A, Cao G, Concas A. **CO2 Absorption in Aqueous NH3 Solutions: Novel Dynamic Modeling of Experimental Outcomes.** *Chemical Engineering Journal* 2023; **415**: 138999.

[31] Álvarez E, Gómez-Díaz D, Navaza JM, Sanjurjo B. **Continuous Removal of Carbon Dioxide by Absorption Employing a Bubble Column.** *Chemical Engineering Journal* 2008; **137**(2): 251–256.

[32] Elavarasan P, Kondamudi K, Upadhyayula S. **Statistical Optimization of Process Variables in Batch Alkylation of p-Cresol with tert-Butyl Alcohol using Ionic Liquid Catalyst by Response Surface Methodology.** *Chemical Engineering Journal* 2009; **155**(1–2): 355–360.

[33] Aslan N, Cebeci Y. **Application of Box–Behnken Design and Response Surface Methodology for Modeling of some Turkish Coals.** *Fuel* 2007; **86**(1–2): 90–97.

[34] Minitab. **Minitab Support.** *Minitab LLC* 2024; **1**: 1.

[35] Mohammad AF, El-Naas MH, Suleiman MI, Al Musharfy M. **Optimization of a Solvay-Based Approach for CO2 Capture.** *International Journal of Chemical Engineering and Applications* 2016; **7**(4): 230-238.

[36] Nakanoh M, Yoshida F. **Gas Absorption by Newtonian and Non-Newtonian Liquids in a Bubble Column.** *Industrial and Engineering Chemistry Process Design and Development* 1980; **19**(1): 190–195.

[37] Grice JV, Montgomery DC. **Design and Analysis of Experiments.** *Technometrics* 2000; **42**(2): 208-215.

[38] Bezerra MA, Santelli RE, Oliveira EP, Villar LS, Escaleira LA. **Response Surface Methodology (RSM) as a Tool for Optimization in Analytical Chemistry.** *Talanta* 2008; **76**(5): 965–977.

[39] Martínez I, Casas PA. **Simple Model for CO2 Absorption in a Bubbling Water Column.** *Brazilian Journal of Chemical Engineering* 2012; **29**(1): 107–111.

[40] Wang B, Lu X, Tao S, Ren Y, Gao W, Liu X, et al. **Preparation and Properties of CO2 Micro-Nanobubble Water Based on Response Surface Methodology.** *Applied Sciences* 2021; **11**(24): 11638.

[41] Descoins C, Mathlouthi M, Le Moual M, Hennequin J. **Carbonation Monitoring of Beverage in a Laboratory Scale Unit with On-Line Measurement of Dissolved CO2.** *Food Chemistry* 2006; **95**(4): 541–553.

[42] Diamond LW, Akinfiev NN. **Solubility of CO2 in Water from −1.5 to 100 °C and from 0.1 to 100 MPa: Evaluation of Literature Data and Thermodynamic Modelling.** *Fluid Phase Equilibria* 2003; **208**(1–2): 265–290.

[43] Zedníková M, Orvalho S, Fialová M, Ruzicka MC. **Measurement of Volumetric Mass Transfer Coefficient in Bubble Columns.** *ChemEngineering* 2018; **2**(2): 19.

[44] Li C, Zhu C, Ma Y, Liu D, Gao X. **Experimental Study on Volumetric Mass Transfer Coefficient of CO2 Absorption into MEA Aqueous Solution in a Rectangular Microchannel Reactor.** *International Journal of Heat and Mass Transfer* 2014; **78**: 1055–1059.